Assessing astrometric quality: stability of the VLBI-derived extragalactic celestial frame

M. Feissel-Vernier

Observatoire de Paris/CNRS UMR8630, 61 Av. de l'Observatoire, 75014, Paris, France
and Institut Géographique National/LAREG

Abstract. This chapter presents background information of a paper (Feissel-Vernier, 2003) that investigated several stable source selection processes and proposed a list of 199 stable sources that could be used for a future improvement of the ICRF. Their performance in maintening the direction of the ICRF axes ($\pm$ 6 μas) is better by a factor of four or five than that of the current 212 ICRF defining sources.

1 Introduction

The wealth of observational data on extragalactic radio sources accumulated by astro-geodetic VLBI in the last two and a half decades makes possible detailed analyses of the time evolution of the radio sources positions. Time series statistics can be used to describe the spectral characteristics of these time evolutions, and to discriminate both stable and unstable sources. Under a deterministic point of view, systematic investigation of apparent linear drifts is also possible. The impact of source motion or instability on the global stability of the celestial reference frame that they materialize can be evaluated.

This study is based on the series of individual source coordinates derived by A. Fey (2002) over 1979-2002.

Section 2 describes the time and space structure of observational data and gives examples of observed time variation of the source coordinates. Section 3 describes the selection scheme applied to detect on the one hand sources that are stable and on the other hand those that are drifting or unstable. The relationship of the resulting set of stable sources with the current ICRF source categories (defining, candidate, other) and the ICRF structure index is examined in section 4. The respective performances of set of sources in maintening the celestial reference frame axes are evaluated in section 5.

2 The observations

The observations consist of time series derived from a set of three analyses of the existing VLBI observing sessions up to May 2002. Each analysis results in time series of coordinates per session for one third of the sources ("arc" sources), the coordinates of the other sources being treated as "global", i.e. they are assumed to stay fixed in time and are estimated globally. Each analysis includes a no-net-rotation (NNR) condition with respect to the ICRF based on the ICRF defining sources.

To avoid inconsistencies that are due to the NNR condition realization in the three analyses, and that can reach the level of 50 microarcseconds (μas), we consider here for each source the time series of its coordinate differences with their global weighted mean.

The frequency bands used in astrometric and geodetic VLBI are the S and X bands, with respective frequencies 2.3 and 8.4 Ghz and wavelengths 13 and 3.6 cm. Figure 1 shows the sky distribution of the most

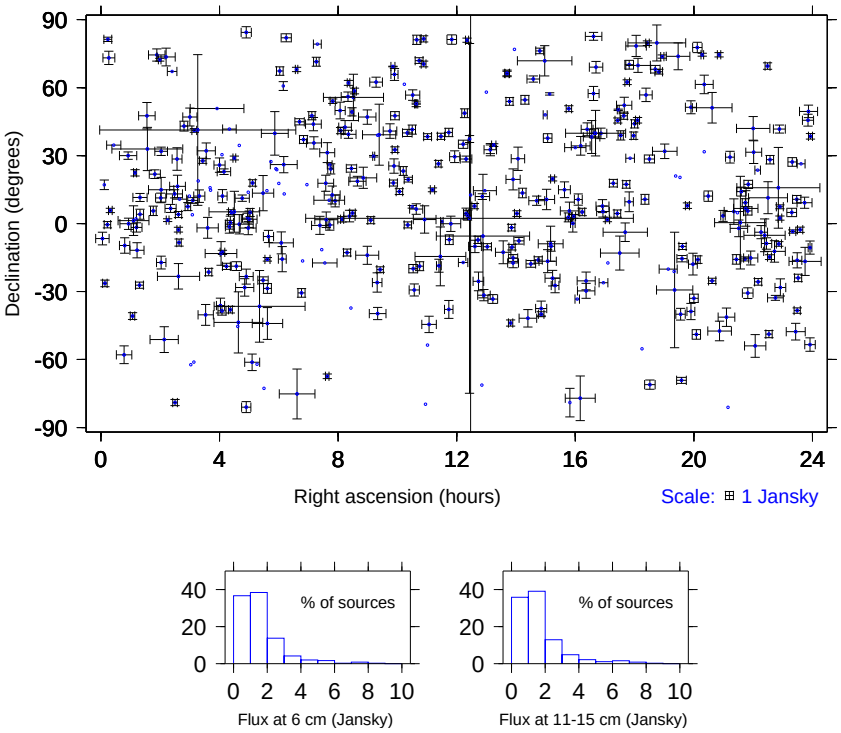

Fig. 1. The most observed ICRF radio sources. Total flux at wavelengths 6 cm (vertical bars), and 11 cm or 15 cm (horizontal bars) is shown when available. Fluxes histograms are shown for sources fainter than 10 Jansky.

observed ICRF sources. The mean flux at 11 or 15 cm, and 6 cm is shown when available at the IERS Celestial Reference System Product Center (IERS 2002).

Figure 2 shows the sky distribution of the most observed sources for one-year time spans centered at the beginning of each year. After a steady extension in the first decade of operation, the sky coverage stabilized during the second one.

Over 700 sources were observed since 1979. The sources observation rates are extremely uneven, as illustrated by the histogram of figure 3. A few sources are observed in nearly all sessions, e.g. 0552+398 has over 205000 observations in over 3000 sessions, while a large number of other sources were observed in less than 20 sessions.

The observed objects are selected by the IVS among quasars and galaxy nuclei that are compact when observed in the X-band and S-band with baseline lengths extending to several thousands kilometers. However, when observed at the current level of precision (a fraction of milliarcsecond, mas), no object is really pointlike. If the source structure is extended or not circular, its apparent direction may change as a function of the length and orientation of the baselines. Most of the known activity of quasars takes the form of jets, i.e., aligned emissive structures that cause an apparent motion of the observed phase center. While the background source structure is assumed to stay fixed, oscillations may exist in the observed direction, as well as apparent drifts that are unlikely to continue indefinitely, but with time characteristics that are not well known. In principle it is possible to accurately correct this effect if repeated maps are available. However, the source structure correction

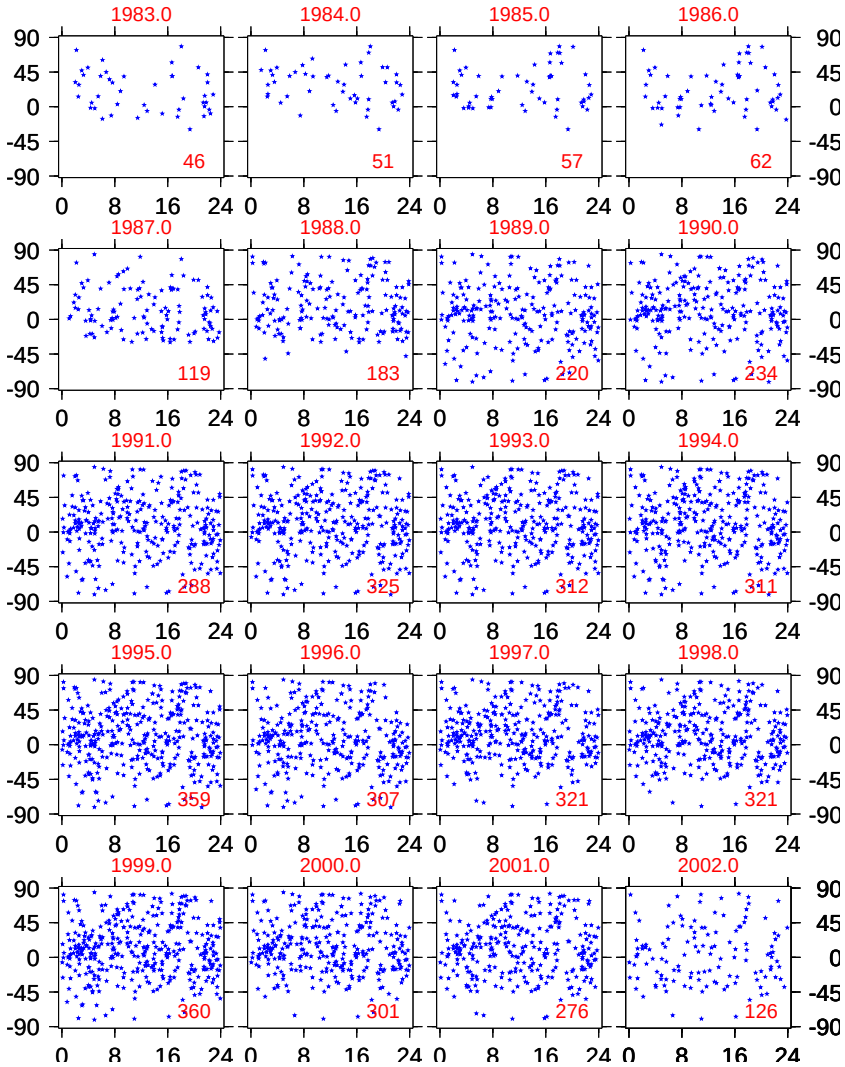

Fig. 2. Year by year sky distribution of the most observed radio sources. The yearly numbers of sources are given in the individual frames.

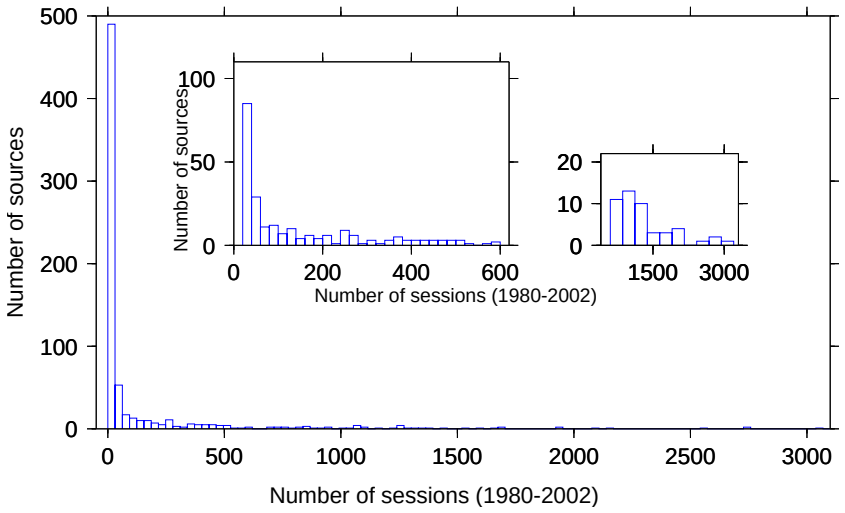

Fig. 3. Observation rates. Number of sessions in which a given source is observed. The leftmost abscissae limit in the right insert is equal

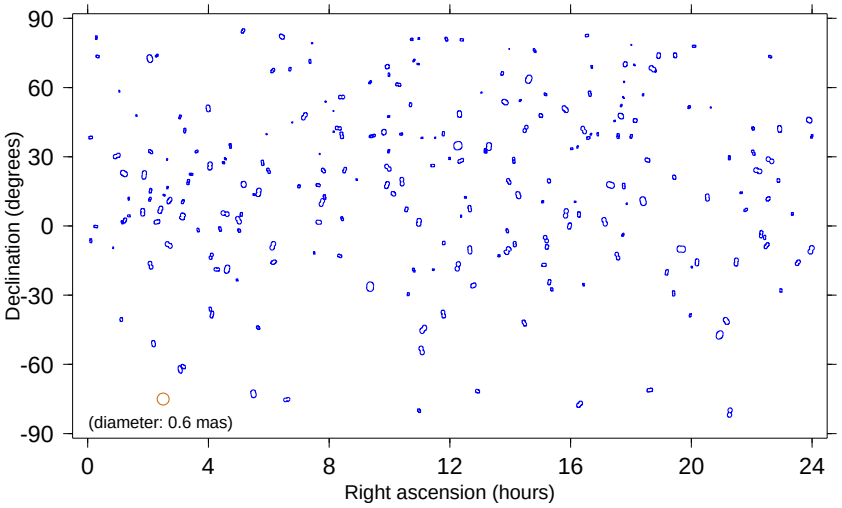

Fig. 4. 245 well observed sources (1989.5-2002.4) with standard deviations of yearly positions smaller than 0.35 mas. Envelops of the standard deviation of the yearly average coordinates in local equatorial frames $(\alpha \cos\delta,\ \delta)$.

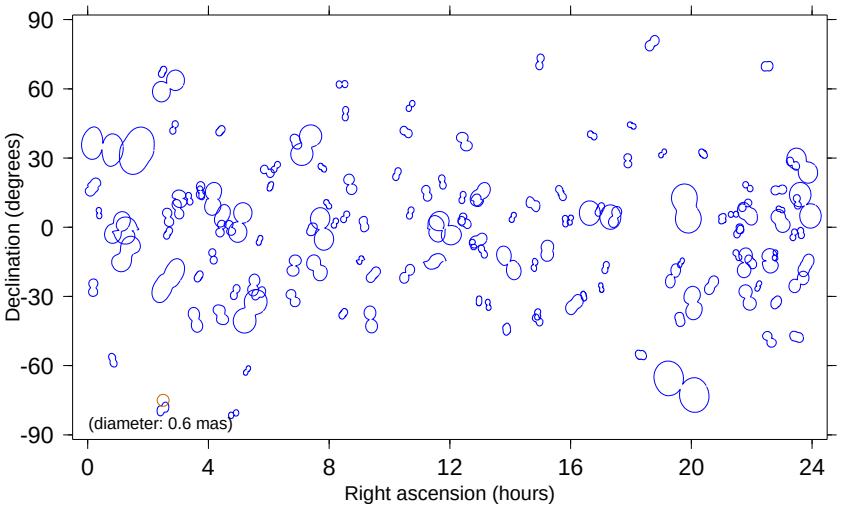

Fig. 5. 143 well observed sources (1989.5-2002.4) with standard deviations of yearly positions larger than 0.35 mas. Envelops of the standard deviation of the yearly average coordinates in local equatorial frames $(\alpha \cos\delta,\ \delta)$.

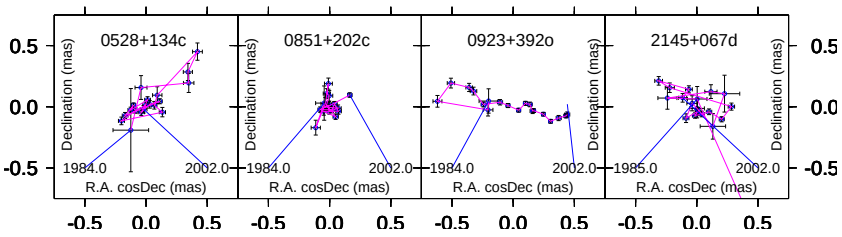

Fig. 6. Observed motion of four radio sources intensively observed over 1984-2002 (yearly averages).

is not implemented in the existing astrogeodetic analysis software. As a result, most objects exhibit time variations of their position in some preferred direction. This is illustrated on Figures 4 and 5, which show the envelopes of the standard deviation of yearly weighted average source positions in local equatorial frames.

Figure 6 shows examples of two-dimensional apparent motions of yearly weighted average source positions in local equatorial frames for four sources: 0528+134 (85517 observations in 2598 sessions), 0851+202, also known as 0J287, (102810 observations in 2788 sessions), 0923+392, also known as 4C39.25, (154589 observations in 2808 sessions), and 2145+067 (61614 observations in 1743 sessions). 0923+392 shows a steady quasi linear motion after 1986, an exceptional situation among the ICRF sources. The other three show a variety of quiet and unquiet behaviours.

Figures 12, 13, 14 and 15 in Annex 1 show the time evolution of the positions of these same four sources in the direction of their maximum variance for 0.1-year weighted average coordinates over 1984-2002. The following comments can be made.

- 0528+134 has a linear drift of 14.8 ± 2.8 μas, with superimposed low frequency oscillations with amplitude of several tens of μas and a high frequency standard deviation equal to 149 μas. The Allan variance analysis (see explanations in section 3) indicates a flicker noise spectrum at the level of 100 μas for sampling intervals up to a few years.
- 0851+202 (0J287) has a slow linear drift (4.8 ± 1.8 μas), with little low frequency oscillations, and a high frequency standard deviation equal to 133 μas. The Allan variance analysis indicates a flicker noise spectrum, also at the level of 100 μas for sampling intervals up to a few years.
- 0923+392 (4C39.25) has a well defined linear drift (57.1 ± 1.4 μas), with relatively strong low frequency oscillations, and a moderate high frequency standard deviation (114 μas). After a flicker noise signal at the level of 100 μas, the Allan variance analysis indicates a random walk for sampling intervals longer than 0.2 years, reaching a level of 300 μas for 5-year sampling times.
- 2145+067 has a slow linear drift (9.0 ± 4.2 μas) and a flicker noise spectrum at a level slightly above 100 μas for sampling intervals up to a few years. Note the large rupture around 1998, raising the high frequency standard deviation to the level of 207 μas.

Apparent source linear velocities give some information on the stability of the sources, at least for the rapidly drifting sources. As an example, a source with a linear drift of 50 μas/year, that would induce a 1 mas source shift after 20 years cannot be considered a "good" source for celestial frame maintenance. Figure 7 shows least-square estimates of source linear drifts over 1989.5-2002.4 as a function of declinations. The inserted histogram shows that a large proportion of sources have apparent drifts smaller than 40 μas/year.

3 The selection scheme

The observational situation is that sources show some level of apparent motions, which may come into contradiction with the basic assumption that, *globally*, the set of selected object has a no net rotation relative

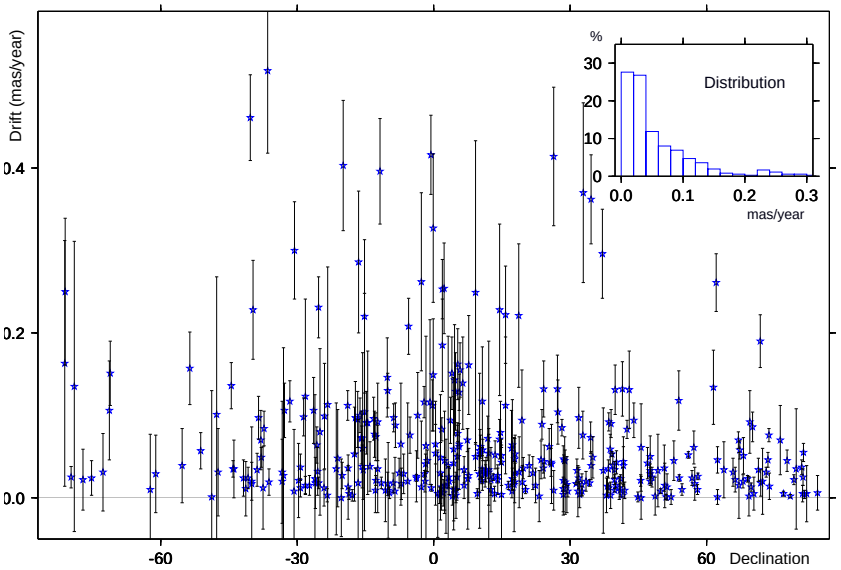

Fig. 7. Sources linear drifts in the direction of maximum variance (1989.5-2002.4), as a function of declination. The insert shows the histogram of the observed drifts.

to the quasi inertial space. However, little is presently known about the actual behaviour of these hundreds of sources, so that a way to solve this difficulty may be to select sources that best match the no-motion model, in order to minimize the uncontrolled global rotation. The authors of the ICRF (Ma et al., 1998) set up three classes of sources, using qualitative and quantitative criteria, such as apparent drift, formal uncertainty of the global coordinates over 1980-1995, source stucture index. They used only the sources they considered as the most reliable (the *defining* sources) for the definition of the ICRF orientation. A second set of apparently reliable sources that had not been enough observed in 1995 were considered as *candidates*. Finally, the remaining sources, considered as unstable, were labelled *other* sources.

The proposed selection scheme is based on a statistical assessment of source stability.

An earlier study (Gontier et al., 2001) had shown that the improvements in VLBI technology, the development of the observing network and the extension of the set of observed objects that took place in operational VLBI, brought the astrometric results to its current precision towards the end of the first decade. Starting about 1990, individual time series of source coordinates stabilize. Therefore, the selection schemes under study are applied to data after 1989.5, i.e. 3.1 million observations of 707 sources, representing 87% of the total observations. Note that values and plots of yearly averages for sources observed since 1984 are available (IERS, 2003).

A set of stable sources is selected in a two-step process, as follows.

1. A first selection is made on the basis of continuity criteria for one-year weighted average coordinates.
   (a) Length of observation period longer than five years.
   (b) Not less than two observations of the source in a given session.
   (c) One-year average coordinates based on at least three observations.

(d) Not more than three successive years with no observations, conditions (b) and (c) being met.
(e) At least half of the one-year averages available over the source observation time span.

This first screening keeps 362 sources for the years centered at 1990.0 through 2002.0. These include 141 defining sources, 130 candidates, 87 other and 4 new sources, i.e. 67% of the defining sources, 44% of the candidates and 85% of the others.

2. The time series of yearly values of $\alpha \cos\delta$ and δ are then analysed in order to derive
   (a) the linear drift (least squares estimation) and the normalized drift. The normalized linear drift is the absolute value of the least-square derived linear drift divided by its formal uncertainty;
   (b) the Allan standard deviation for a one-year sampling time. The Allan variance of a time series x_i with N items and sampling time τ is defined as:

$$\sigma_A^2(\tau) = \frac{1}{2N} \sum_i (x_{i+1} - x_i)^2$$

The Allan variance analysis (Allan, 1966), see a review of these methods in (Rutman, 1978)) allows one to characterize the power spectrum of the variability in time series, for sampling times ranging from the initial interval of the series to 1/4 to 1/3 of the data span, in our case one year through four years. This method allows one to identify white noise (spectral density S independent of frequency f), flicker noise (S proportional to f^{-1}), and random walk (S proportional to f^{-2}). Note that one can simulate flicker noise in a time series by introducing steps of random amplitudes at random dates. In the case of a white noise spectrum (an implicit hypothesis in the current ICRF computation strategy), accumulating observations with time eventually leads to the stabilisation of the mean position. In the case of flicker noise, extending the time span of observation does not improve the quality of the mean coordinates.

The distributions of the above statistics applied to the 362 preselected sources are shown on figure 8.

Based on these statistics, rules are set up to derive source stability indices. For each local coordinate ($\alpha \cos\delta$ and δ), three partial indices are defined, as shown in Table 1. The thresholds are set after the distributions of figure 8. The partial stability indices range from 1 (most stable) through 3 (least stable). A rejection value (10) is associated to very large drifts or standard deviations. Given the length of the available time series (up to 13 years), one could consider the Allan standard deviation for sampling times longer than one year (e.g. two or four years). The one-year interval is preferred because its estimation is expected to be more robust than for longer time spans.

The partial stability criteria derived by applying the thresholds of Table 1 are then combined in five different ways, each one representing a different balance in the roles of the standard deviations and the drifts. Fifty sources were found to have apparent drifts larger than 50 μas/year. They are excluded a priori in the five options.

We reproduce in Annex 2 the table giving detailed statistics on the 362 sources well observed over 1989.5-2002.4, taken from Feissel-Vernier (2003), which is published only in electronic form in A&A.

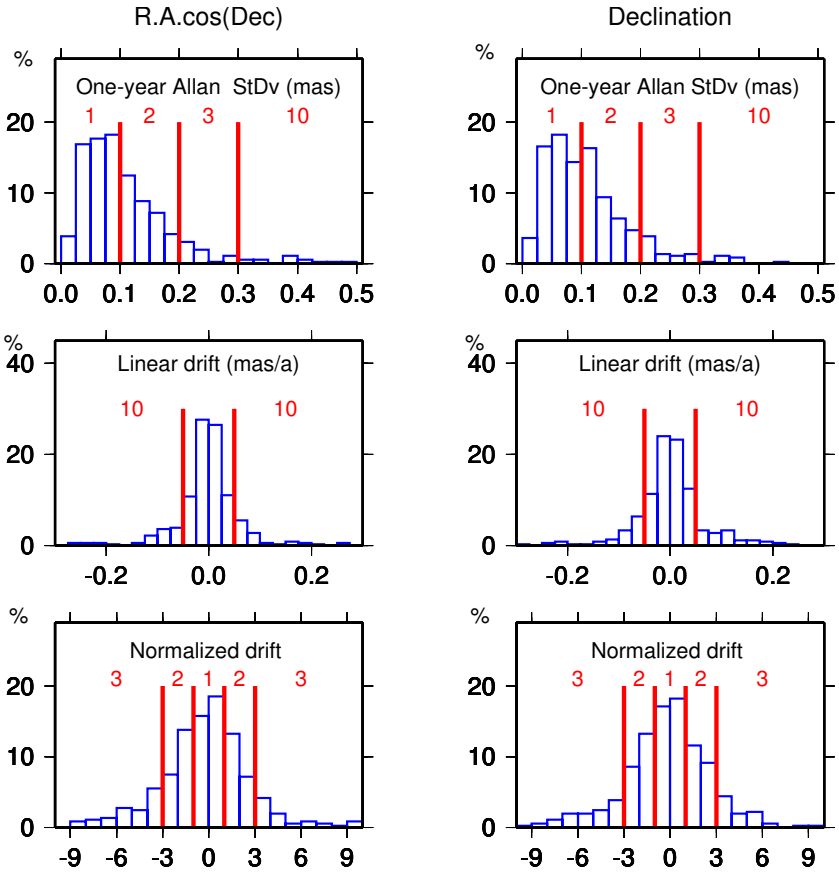

Fig. 8. Distributions of the partial stability criteria for the well observed sources over 1989.5-2002.4. The thresholds and corresponding partial indices listed in Table 1 are shown.

Table 1. Partial stability criteria. The values range from 1 (best) through 3 (worse), with a rejection value of 10.

Statistics	Threshold	Partial index
Allan Standard deviation (AlSd)		
	AlSd $\leq$ 100 μas	1
	100 μas $\leq$ AlSd $\leq$ 200 μas	2
	200 μas $\leq$ AlSd $\leq$ 300 μas	3
	AlSd $\geq$ 300 μas	10
|Drift| (Vel)		
	Vel $\leq$ 10 μas/year	1
	Vel $\geq$ 50 μas/year	10
|Normalized drift| (Nvl)		
	Nvl $\leq$ 1	1
	1 $\leq$ Nvl $\leq$ 3	2
	Nvl $\geq$ 3	3

4 Relationships of the stable sources with the ICRF source qualification

The **partial stability indices** for each of the 362 sources investigated (drift, Allan variance and normalized drift) can be compared with two existing ICRF qualifiers:

- the source status: defining, candidate or other, and
- the source structure index in the X band when available. Structure index values 1 and 2 indicate very good and good astrometric suitability, values 3 and 4 poor and very poor suitability.

The comparison with the source status is plotted in figure 9 for the 312 well observed sources with apparent drifts smaller than 50 μas/year over 1989.5-2002.4. The graphs give the positions of the defining, candidate and other sources as a function of both the one-year Allan standard deviation and the normalized drift. Although a number of defining sources fall in the lower-left zone which correspond to small partial stability indices, some of them are clearly detected as unstable. The candidate sources are globally in the same situation. Conversely, a number of 'other' sources, i.e. considered as having questionable stability in the ICRF work, are detected as stable. Compared to the ICRF selection, the proposed scheme rescues a number of sources that are in fact efficient for maintaining the ICRF axes directions.

The comparison with the source structure indices, plotted on figure 10, also shows moderate cross correlation of the two types of criteria.

Table 2 gives the relationship of the **global stability index** with the ICRF qualifiers. Sources with global stability indices 1 and 2 are considered as stable. Although a number of defining sources get small, i.e. good, partial stability indices, some of them are clearly detected as unstable. The candidate sources are globally in the same situation. Conversely, a number of 'other' sources, i.e. considered as having questionable stability in the ICRF work, are detected as stable. Compared to the ICRF selection, the proposed scheme rescues a number of sources that are in fact efficient for maintaining the ICRF axes directions. For what concerns the source stability indices, 80% of the stable sources have a good structure index (1 or 2), while the ratio is also large for the unstable sources (64%). Altogether, 61% of the well observed sources with a good structure index are detected as stable, and 39% are detected as unstable. This finding is of interest in the context of studying the dynamics of the quasars activity. Similarly, there is no clear relationship of the source total fluxes in the X and S bands with their direction time variability. A possible relationship with the flux variability remains to be investigated.

Figure 11 shows the sky distribution of the proposed stable and unstable sources, together with that of the current ICRF defining sources.

5 Testing source selections

Out of the 362 preselected sources the proposed stability scheme produces 199 stable sources, a number to be compared to the 212 defining sources in the ICRF. To test their efficiency with respect to the maintenance of the axes of the celestial reference frame that they materialize, we consider the 13 yearly differential reference frames (1990.0 - 2002.0) that are formed by the coordinates of the stable sources observed in

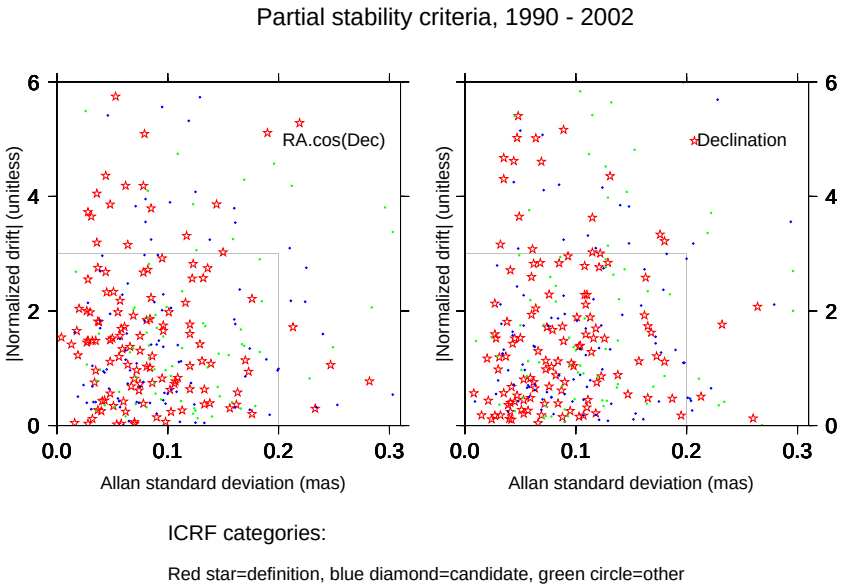

Fig. 9. Partial stability criteria and ICRF source classes

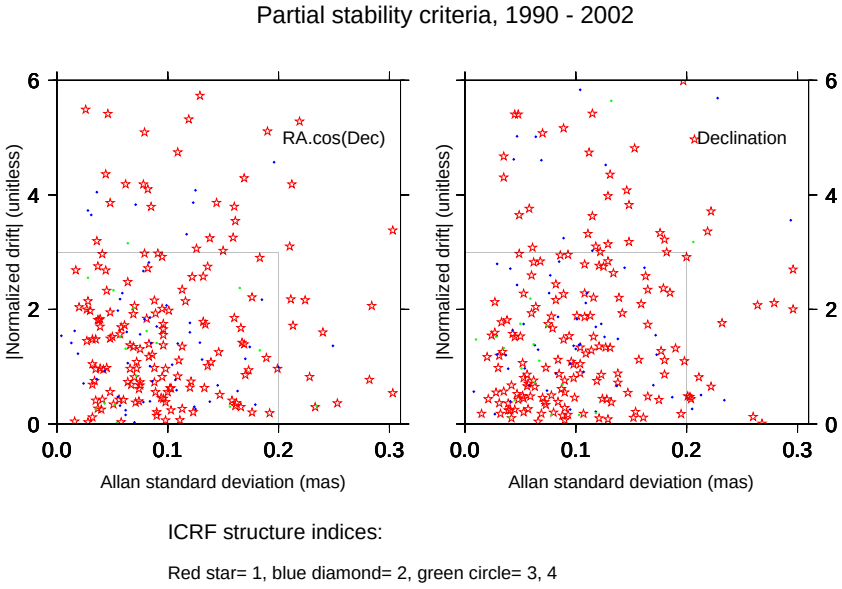

Fig. 10. Partial stability criteria and ICRF source source structure index

Table 2. Stability index and ICRF source qualifiers

Stab.	Source status			Structure index		
index	Def.	Can.	Oth.	1	2	3-4
1	33	26	15	46	11	7
2	48	42	34	76	26	6
3	2	1	4	6	2	0
4	58	61	34	70	26	13

Table 3. Stability test

Source selection scheme	Nb of sources kept	Std dev. μas	Allan Std dev. 1 year μas	4 years μas
Stable	199	10.8	9.4	5.9
ICRF Defining	212	25.6	26.0	27.6

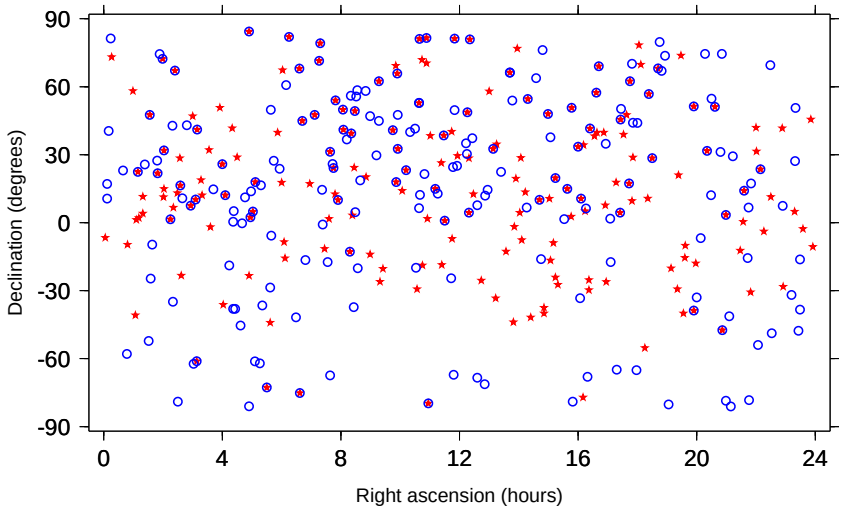

Fig. 11. Detected stable sources (stars) over 1989.5-2002.4 and ICRF defining sources (circles).

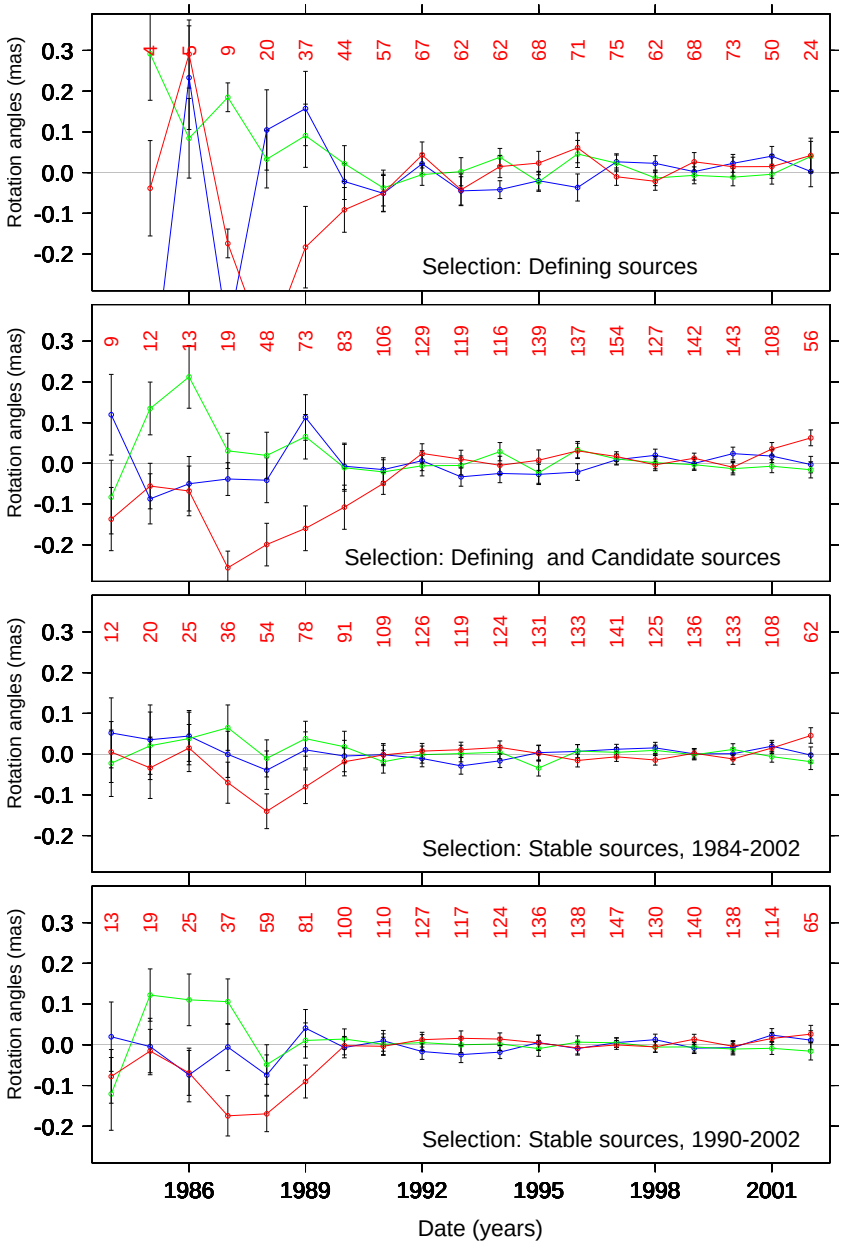

Fig. 12. Rotation angles of yearly differential reference frames - A1: blue (dark) - A2: green (light) - A3: red (medium) - Unit: 0.001" (mas). The numbers of selected sources for each year are given.

each year. The yearly differential rotation angles $A_1(y)$, $A_2(y)$, $A_3(y)$ around the axes of the equatorial coordinate system for year y are then computed for the 13 years.

Table 3 lists efficiency estimates for the stability scheme and for the ICRF defining sources. These estimates are the usual standard deviation that characterizes the scattering of the sets of rotation angles, and their Allan standard deviations for one-year and four-year sampling times, that characterize their stability in time. Note that if the time series of the rotation angles have white noise, the four-year Allan standard deviation will be equal to half (square root of one fourth in sampling time) the one-year one. In the case of flicker noise, both values will be equal.

The estimated efficiency of the ICRF defining sources is worse than that of the proposed selection by nearly a factor of three for the one-year estimates and a factor of five in the longer term.

6 Discussion

When compared to the current ICRF defining sources, the selection scheme developed in this study achieves improved time stability of yearly reference frames, which implies improved internal consistency. This has consequences not only in astrometric applications, but it may also have bearings in the geophysical interpretation of the Earth's orientation in inertial space. As an example, Dehant et al. (2002) have shown that source instabilities perturb precession and long term nutation determinations at the level of tens of μas, a level comparable to that of the discrepancy of VLBI results with the precession constant or the 18.6-year nutation component in the IAU2000 Nutation model.

Finally, we recommend that the set of selected stable sources be considered on the one hand in any future improvement of the International Celestial Reference Frame, and on the other hand in the scheduling of repeated VLBI sessions for Earth rotation, geodesy and astrometry.

Acknowledgements. The data analysis in this study is entirely based on the time series of coordinates of 707 radio source derived by Alan Fey (USNO) using 3.6 millions of observations accumulated in various US and international programs since 1979.

References

Allan, D. W. 1966, Proc. IEEE 54, 221

Dehant, V., Feissel-Vernier, M., de Viron, O., Ma, C., Yseboot, M., Bizouard, C., 2002, JGRB, 108, 2275, DOI 2002JB001763.

Feissel-Vernier, M., 2002, anonymous ftp: ftp://lareg.ensg.ign.fr/pub/martine/crono_vue

Feissel-Vernier, M., 2003, A&A, 403, 105

Fey, A. L., 2002, Private communication

Fey, A. L., Charlot, P., 2000, ApJS 128, 17

Gontier, A.-M., Le Bail, K., Feissel, M., 2001, A&A 375, 661

IERS 1999, ftp://hpiers.obspm.fr/icrs-pc/icrf/iau/icrf-Ext.1

IERS 2002, ftp://hpiers.obspm.fr/icrs-pc/icrf/iau/icrf.car

IERS 2003, http://hpiers.obspm.fr/icrs-pc/icrf/time-series.html

Ma, C., Arias, E. F., Eubanks, T. M., Fey, A. L., Gontier, A.-M., Jacobs, C. S., Sovers, O. J., Archinal, B. A., Charlot, P., 1998, AJ 116, 516

Rutman, J., 1978, Proc. IEEE 66, 1048

7 Annex 1

Time series of source displacement, 1984-2002

- Figure 13: 0528+134
- Figure 14: 0851+202
- Figure 15: 0923+392
- Figure 16: 2145+067

8 Annex 2

We reproduce hereafter the table giving detailed statistics on the 362 sources well observed over 1989.5-2002.4, taken from Feissel-Vernier (2003, referred to as MFV hereafter), which is published only in electronic form in A&A.

The redshift and the total flux at 6 cm, 11/15 cm are given when available. 'AlSd' is the Allan standard deviation for a one-year sampling time.

1. The ICRF source status: d = defining, c = candidate, o = other, n = not available in ICRF Ext-1.
2. The source structure index, when available in ICRF-Ext.1. This index (Fey and Charlot, 2000) qualifies the level of position disturbance expected as a result of the the source structure (1 for the least disturbed, 4 for the most disturbed)
3. The stability index derived in MFV; values 1 and 2 correspond to stable sources, 3 to unstable, and 4 to highly unstable or drifting. The stability indices are rounded off.
4. The same stability criterion as above, but keeping only yearly averages based on at least twelve observations (instead of three).

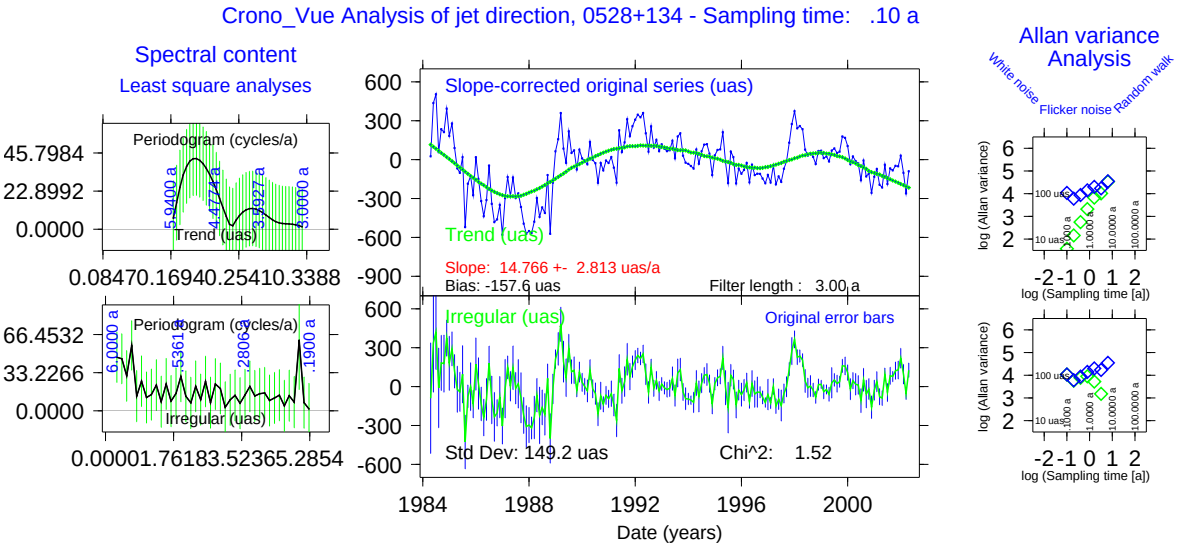

Fig. 13. Time series at 0.1-year intervals showing the apparent motion of source 0528+134 in the direction of maximum variance.

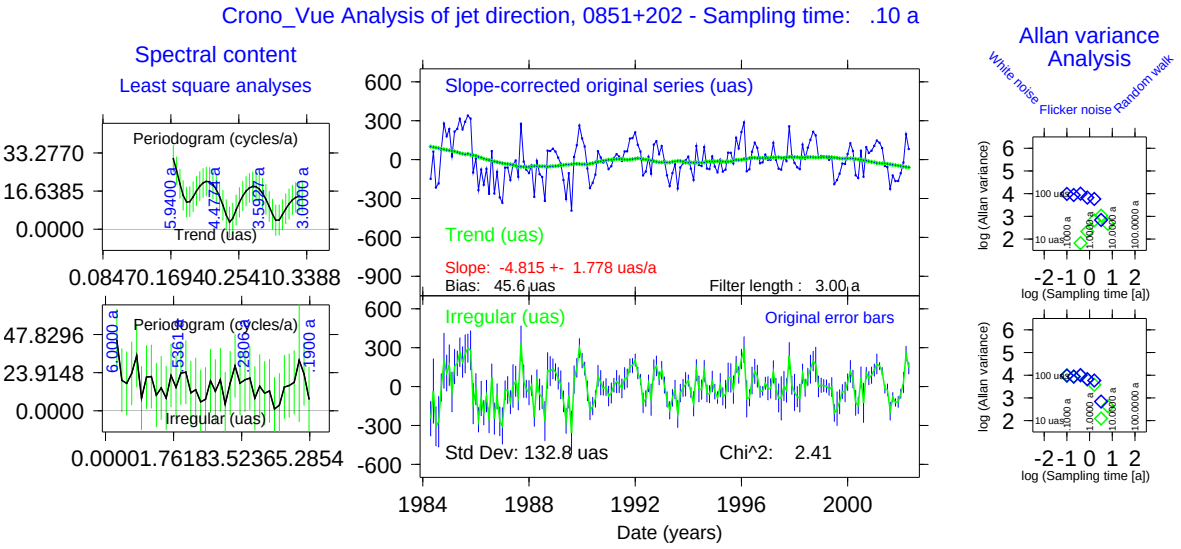

Fig. 14. Time series at 0.1-year intervals showing the apparent motion of source 0851+202 (OJ287) in the direction of maximum variance.

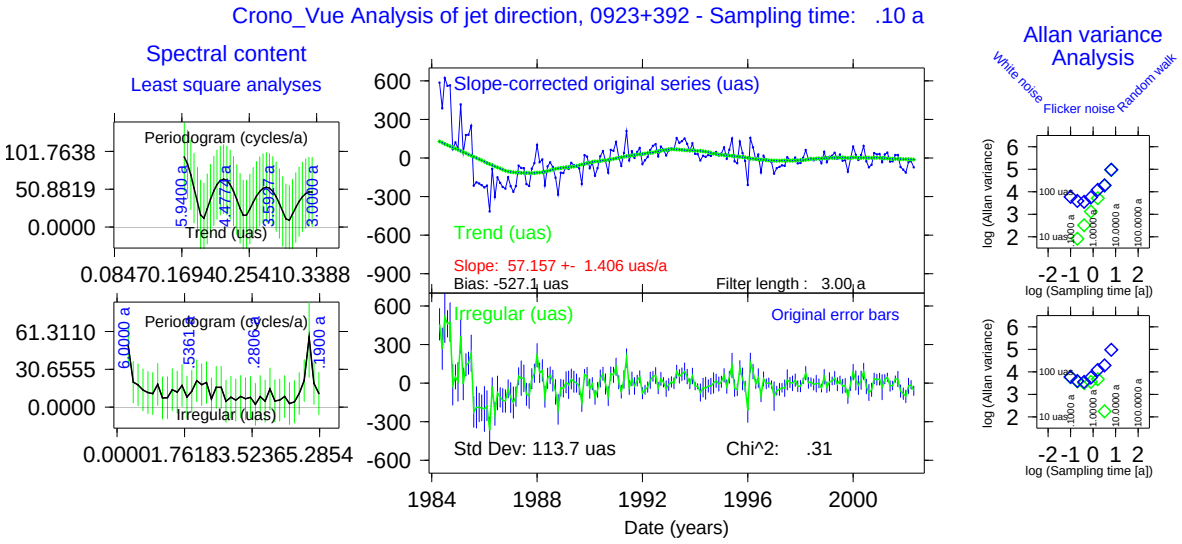

Fig. 15. Time series at 0.1-year intervals showing the apparent motion of source 0923+392 (4C39.25) in the direction of maximum variance.

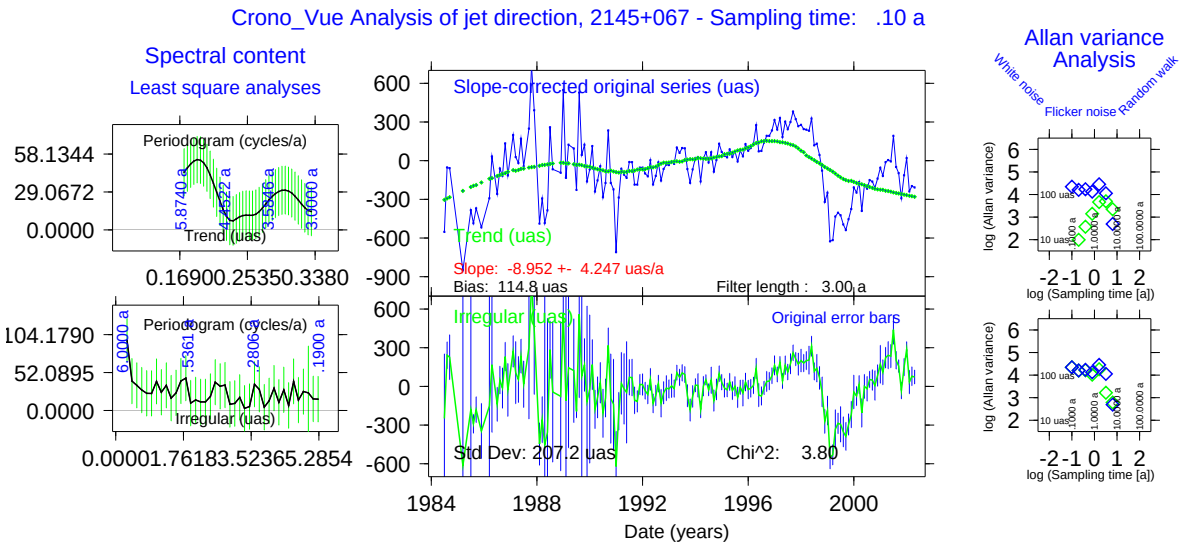

Fig. 16. Time series at 0.1-year intervals showing the apparent motion of source 2145+067 in the direction of maximum variance.

Table 4. Stability criteria for 362 well observed extragalactic sources, 1989.5-2002.4

No	Source	Alter.	Redsh.	Flux (Jy) 6 cm	11 cm	15 cm	Number sess	pts	R.A. cos(δ) AlSd μas	Drift μas/year	Declination AlSd μas	Drift μas/year	Stability criteria 1	2	3	4
1	0003 + 380		.23	.5		.6	12	8	32	-2 ± 20	15	-2 ± 11	d	1	1	1
2	0003 − 066		.35	1.6		1.7	492	12	110	-9 ± 8	177	30 ± 24	c	1	2	2
3	0007 + 171		1.60	1.2	.9		14	7	44	-66 ± 15	41	7 ± 31	d	1	4	
4	0008 − 264		1.09	.8		.6	12	9	19	-50 ± 13	64	101 ± 39	c		4	
5	0013 − 005		1.57	.8	.8		54	11	597	15 ± 4	70	4 ± 10	c	1	4	4
6	0014 + 813		3.39	.6		1.0	449	11	96	-7 ± 4	207	54 ± 11	d	1	4	4
7	0016 + 731		1.78	1.6		1.5	425	12	169	-26 ± 6	134	-15 ± 6	o	1	2	2
8	0019 + 058			.5	.5		27	9	26	-35 ± 6	112	-154 ± 32	o	1	4	
9	0026 + 346		.52			1.8	12	5	98	-393 ± 52	10	38 ± 26	o	4	4	
10	0048 − 097			1.9		1.3	1058	13	83	-5 ± 3	104	-7 ± 7	o	1	1	1
11	0056 − 001		.72	1.4		2.2	12	8	136	-262 ± 51	94	194 ± 90	c	3	4	
12	0059 + 581						932	11	158	2 ± 5	197	-26 ± 4	o	1	2	2
13	0104 − 408		.58	.9	.6		499	13	81	-4 ± 12	71	23 ± 13	o		1	1
14	0106 + 013		2.11	3.7		3.9	1280	13	69	6 ± 5	93	1 ± 9	o	1	1	1
15	0109 + 224			.8	.4		14	9	72	24 ± 25	30	13 ± 13	d	1	1	1
16	0111 + 021		.05				167	12	39	-16 ± 9	39	-3 ± 13	c	1	1	1
17	0112 − 017		1.37	1.2	1.4		49	10	192	68 ±117	79	58 ± 40	c	1	4	4
18	0113 − 118		.67	1.9	1.8		27	9	179	-31 ± 93	117	-313 ± 49	o	2	4	4
19	0119 + 041		.64	1.2		.9	1427	13	192	2 ± 11	161	-1 ± 7	c	1	2	2
20	0119 + 115		.57	1.0		1.8	387	11	45	4 ± 4	179	-34 ± 14	c	1	2	2
21	0133 + 476		.86	3.3		2.1	500	13	136	-14 ± 5	68	-12 ± 4	d	1	2	2
22	0134 + 329	3C48	.37	5.4	9.0		11	5	88	56 ±159	85	-299 ±189	o	4	4	
23	0146 + 056		2.35	1.2	.7		54	10	28	32 ± 15	89	63 ± 28	c	1	4	4
24	0149 + 218		1.32	1.1		1.4	43	9	107	-10 ± 13	104	30 ± 22	d	2	2	2
25	0159 + 723			.3	.3		19	7	37	-7 ± 26	84	-16 ± 41	d	1	1	1
26	0201 + 113		3.61	1.2		1.3	360	13	91	21 ± 7	131	-22 ± 16	c	1	2	2
27	0202 + 149		.41	3.1		3.2	516	13	174	-9 ± 7	228	49 ± 9	c	2	2	2
28	0202 + 319		1.47	1.0		1.6	40	11	55	-19 ± 10	41	-4 ± 11	d	2	1	1
29	0208 − 512		1.00	3.2	3.6		274	13	140	3 ± 17	127	-58 ± 21	o		4	4
30	0212 + 735		2.37	2.2		2.3	1264	12	196	36 ± 8	127	-27 ± 6	o	2	3	3
31	0215 + 015		1.72	.4	.4		23	9	173	34 ± 36	87	11 ± 18	d	1	1	1
32	0221 + 067		.51	1.0		1.4	45	9	85	20 ± 14	29	-44 ± 16	c	2	2	2
33	0224 + 671	4C67.05				1.2	40	7	74	20 ± 32	90	28 ± 37	d	1	1	1
34	0229 + 131		2.07	1.0		2.0	1946	13	105	-23 ± 3	125	-11 ± 4	c	1	2	2
35	0230 − 790		1.07	.8	.6		11	7	70	10 ±170	43	-129 ± 91	d		4	
36	0234 + 285		1.21	2.8	1.2		1085	12	49	11 ± 1	123	-5 ± 3	c	2	2	2
37	0235 + 164		.94	2.8		2.0	442	13	103	1 ± 4	121	-14 ± 5	d	1	2	2
38	0237 + 040		.98	.8		.8	22	8	56	8 ± 18	118	140 ± 45	c	1	4	4
39	0237 − 027		1.12	.6	.4		14	8	174	137 ±102	104	-209 ± 65	c	1	4	4
40	0237 − 233		2.22	3.2	5.3		13	7	52	-20 ± 62	78	22 ±140	o	3	1	
41	0238 − 084	NGC1052	.00	.9	.6		275	10	123	-87 ± 22	138	-38 ± 26	o	2	4	4
42	0239 + 108					1.8	83	12	78	28 ± 11	44	-62 ± 13	d	2	4	4
43	0248 + 430		1.31	1.2	1.0		13	7	84	-47 ± 25	115	122 ± 40	d	2	4	4
44	0256 + 075		.89	1.0		.7	38	8	95	26 ± 32	72	21 ± 55	d	1	1	
45	0300 + 470			2.2	1.8		716	12	166	-15 ± 9	296	36 ± 18	o	1	2	4
46	0302 − 623						18	6	81	59 ± 58	51	-17 ± 60	d		4	4
47	0306 + 102		.86	.7		1.3	30	9	96	40 ± 23	79	-37 ± 22	d	1	2	2
48	0308 − 611						80	8	133	17 ± 45	73	30 ± 26	d		2	2
49	0309 + 411		.14	.5		.6	12	6	13	-12 ± 8	69	22 ± 5	d	2	2	
50	0317 + 188						30	6	32	16 ± 15	56	-27 ± 41	c	1	1	

(continued on next page)

(Table 4. continued)

No	Source	Alter.	Redsh.	Flux (Jy) 6 cm	11 cm	15 cm	Number sess	pts	R.A. cos(δ) AlSd μas	Drift μas/year	Declination AlSd μas	Drift μas/year	Stability criteria 1	2	3	4
51	0319+121		2.67	1.5		1.4	20	10	35	-5 ± 20	51	40 ± 42	o	3	1	1
52	0332–403		1.45	2.6	1.9		11	7	129	-147 ± 30	212	-426 ± 55	o		4	
53	0333+321	NRAO140	1.26	2.0		2.3	80	10	72	-11 ± 13	67	-11 ± 10	o	3	1	1
54	0336–019	CTA26	.85	2.6		2.7	726	13	160	16 ± 8	279	-25 ± 12	c	1	2	2
55	0338–214		.05	.9	.8		29	7	101	-124 ± 77	126	-87 ± 71	o		4	4
56	0341+158						22	7	50	-39 ± 6	104	110 ± 82	c	1	4	
57	0342+147						32	10	59	-50 ± 11	176	-69 ± 37	d	1	4	4
58	0355+508	NRAO150				6.8	470	9	43	6 ± 16	88	-20 ± 28	o	3	1	1
59	0400+258		2.11	1.8		1.4	36	9	120	26 ± 15	85	46 ± 16	d	2	2	2
60	0402–362		1.42	1.9	1.0		344	13	38	-14 ± 9	57	-18 ± 16	o		2	2
61	0403–132		.57	2.9		4.0	11	6	23	-49 ± 6	49	88 ± 29	o	1	4	
62	0405–385		1.28	1.1		1.0	73	9	19	13 ± 26	44	97 ± 23	c		4	
63	0406+121		1.02	1.6	1.2		32	9	75	-29 ± 40	260	20 ±156	d	1	2	2
64	0406–127		1.56	.5	.6		16	7	79	-8 ± 3	159	69 ± 33	c	1	4	
65	0414–189		1.54	.8		1.0	11	6	125	113 ± 18	19	-43 ± 5	d	1	4	
66	0420+417					1.7	19	8	63	-36 ± 22	39	23 ± 24	c	2	1	
67	0420–014		.92	1.6		1.0	1247	11	228	-10 ± 12	222	-45 ± 12	o	1	3	3
68	0422+004			1.6		.8	18	8	48	-15 ± 26	98	61 ± 58	d	1	4	4
69	0422–380		.78	.8	.5		15	8	28	-29 ± 20	32	89 ± 28	d		4	
70	0425+048						16	7	34	52 ± 59	24	174 ± 38	c	3	4	
71	0430+052	3C120	.03	5.1		6.4	97	9	183	-50 ± 39	50	-18 ± 10	o	3	4	4
72	0430+289			.5	.4		33	5	27	30 ± 28	71	-4 ± 29	n		1	1
73	0434–188		2.70	1.1		1.3	92	12	82	56 ± 14	99	17 ± 37	o	1	4	4
74	0440+345						30	10	41	15 ± 5	148	72 ± 19	c	1	4	4
75	0440–003	NRAO190	.84	2.4	3.5		18	7	40	-61 ± 15	40	-95 ± 37	d	1	4	
76	0451–282		2.56	2.2		2.3	11	7	78	-48 ± 63	124	104 ±106	c		4	
77	0454+844		$\geq$ 1.34	1.4		1.3	58	11	139	-14 ± 13	116	-25 ± 17	d	1	2	2
78	0454–234		1.00	1.9	1.8		1600	13	136	7 ± 7	124	3 ± 6	o	1	2	2
79	0454–810		.44	1.4	1.2		20	7	65	-218 ± 85	29	113 ± 26	d		4	
80	0457+024		2.38	1.2		1.3	59	11	57	29 ± 19	66	-1 ± 30	d	1	1	1
81	0458–020		2.29	1.6		2.0	1256	13	211	-16 ± 7	200	-21 ± 7	c	1	3	3
82	0500+019		.58	2.0		2.0	16	9	223	-54 ± 16	317	246 ± 62	o	3	4	4
83	0502+049		.95	1.0		.6	11	6	4	9 ± 6	8	-9 ± 15	d	2	1	
84	0507+179		.42	.8		.7	42	12	120	-35 ± 22	95	-6 ± 23	d	2	2	2
85	0521–365		.05	8.9		11.5	90	11	488	261 ± 82	342	-446 ± 87	d		4	
86	0528+134		2.07	4.4	2.7		2546	13	469	-7 ± 8	198	4 ± 4	c	1	4	4
87	0528–250		2.77	.8	1.3		16	8	56	-18 ± 31	120	88 ±102	o		4	
88	0530–727						55	7	43	-13 ± 29	76	32 ± 47	d		1	1
89	0536+145						33	7	96	-18 ± 12	58	-74 ± 20	o	1	4	4
90	0537–286		3.10	1.2		1.0	19	9	90	74 ± 35	52	-59 ± 19	d		4	
91	0537–441		.90	4.0	3.8		360	13	109	39 ± 8	82	24 ± 11	o	1	2	2
92	0539–057		.84	1.5	1.3		12	8	50	63 ± 41	39	32 ± 88	d	1	4	
93	0544+273						34	7	70	-17 ± 21	163	-101 ± 39	d	1	4	4
94	0552+398		2.36	5.4		3.4	3039	13	129	-8 ± 1	148	-5 ± 2	c	1	2	2
95	0554+242						22	5	42	-112 ± 36	173	-99 ± 83	n		4	4
96	0556+238						245	12	95	-35 ± 12	131	-75 ± 17	d	1	4	
97	0600+177						11	6	100	-22 ± 39	98	-34 ± 42	c	1	1	
98	0602+673		1.97	1.1	.8		13	7	85	38 ± 12	66	-48 ± 6	c		2	2
99	0605–085		.87	2.7	3.0		27	9	42	-16 ± 17	57	-25 ± 35	c	1	1	1
100	0607–157		.32	3.1		1.0	22	9	109	-36 ± 26	63	19 ± 14	c	2	2	4

(continued on next page)

(Table 4. continued)

No	Source	Alter.	Redsh.	Flux (Jy) 6 cm	11 cm	15 cm	Number sess	pts	R.A. cos(δ) AlSd μas	Drift μas/year	Declination AlSd μas	Drift μas/year	Stability criteria 1	2	3	4
101	0615 + 820		.71	1.0		1.3	30	8	51	-9 ± 25	60	35 ± 18	d	1	1	1
102	0636 + 680		3.18	.5	.3		34	9	30	15 ± 7	64	-17 ± 8	d	1	2	2
103	0637 − 752		.65	6.2	4.5		277	13	247	-23 ± 21	109	16 ± 10	d		2	2
104	0642 + 449		3.41	.8		1.2	464	12	113	2 ± 6	69	-1 ± 3	d	1	1	1
105	0646 − 306		.46	1.1		.9	11	6	39	170 ± 42	41	172 ± 86	c	2	4	
106	0648 − 165						17	7	109	-30 ± 35	115	192 ± 53	d	1	4	4
107	0650 + 371		1.98	1.0		1.0	30	7	192	-249 ± 45	109	-202 ± 58	c	1	4	4
108	0657 + 172						114	12	88	-14 ± 7	85	-6 ± 7	c	1	1	1
109	0707 + 476		1.29	1.0		.8	13	7	150	-26 ± 8	165	45 ± 26	d	1	2	2
110	0716 + 714			1.1		.7	94	10	38	-12 ± 7	108	-33 ± 15	d	1	2	2
111	0718 + 7920718+793					1.0	476	10	78	23 ± 5	57	1 ± 4	d	1	2	2
112	0723 − 008		.13	2.3		2.1	27	8	163	45 ± 77	173	-94 ± 77	d	2	4	4
113	0727 − 115						2101	13	159	12 ± 4	165	16 ± 7	o	1	2	2
114	0735 + 178		≥ .42	2.0		2.0	486	12	377	-40 ± 25	180	-10 ± 12	o	1	4	4
115	0736 + 017		.19	1.9		2.9	43	11	234	4 ± 13	35	18 ± 13	c	3	2	2
116	0738 + 313		.63	2.5		1.9	22	9	144	-6 ± 2	80	-15 ± 2	d	1	2	2
117	0742 + 103					3.9	301	12	126	39 ± 13	129	-52 ± 13	o	1	4	4
118	0743 + 259					.6	18	9	176	-14 ± 71	122	122 ± 41	d	1	4	
119	0743 − 006		.99	1.3	1.0		24	9	116	-95 ± 31	289	-412 ± 45	o	1	4	
120	0745 + 241		.41	1.3	.7		111	10	57	-20 ± 9	47	-32 ± 6	d	2	2	2
121	0748 + 126		.89	2.2		2.0	20	7	24	8 ± 11	74	22 ± 38	c	2	1	1
122	0749 + 540		≥ .20	.6	.7		376	12	141	-27 ± 4	96	-4 ± 3	d	1	2	2
123	0754 + 100		.28	1.5	1.0		20	8	27	-28 ± 14	47	-11 ± 21	d	1	1	1
124	0804 + 499		1.43	2.1		1.3	768	13	101	6 ± 3	101	-5 ± 3	d	1	2	2
125	0805 + 410		1.42	.8		.7	240	11	67	-5 ± 7	53	4 ± 5	d	1	1	1
126	0808 + 019			.7		.4	28	8	199	86 ± 25	247	-228 ± 37	c	1	4	4
127	0814 + 425		.26	1.7		1.6	116	11	165	-82 ± 11	75	-11 ± 6	c	1	4	4
128	0818 − 128			.9		.9	18	7	86	29 ± 24	35	-11 ± 20	d	1	1	
129	0820 + 560		1.42	1.2		1.7	53	11	29	52 ± 4	27	4 ± 3	d	1	4	4
130	0821 + 394		1.22	1.0		1.9	14	8	19	-8 ± 6	41	-39 ± 14	d	2	1	1
131	0821 + 621		.54	.6	.3		12	6	218	-261 ± 35	90	38 ± 20	c		4	4
132	0823 + 033		.51	1.4		1.4	785	13	161	-21 ± 6	190	-17 ± 13	c	1	2	2
133	0826 − 373						16	9	53	-77 ± 13	24	-2 ± 22	d		4	
134	0827 + 243		.94	.9		1.3	62	10	108	-8 ± 13	162	47 ± 17	c	2	2	2
135	0828 + 493		.55	1.0		.5	14	8	16	0 ± 11	62	33 ± 44	d	1	1	1
136	0829 + 046		.18	.7		.7	14	7	123	-93 ± 34	133	111 ± 61	d	2	4	4
137	0839 + 187		1.27	1.2		2.2	21	10	140	52 ± 21	363	218 ± 85	d	3	4	4
138	0851 + 202	OJ287	.31	2.6	3.4		2756	13	224	9 ± 4	121	5 ± 3	c	1	2	2
139	0859 − 140		1.34	2.3		2.9	18	7	57	46 ± 31	62	36 ± 26	c	3	2	4
140	0906 + 015		1.02	.9		.8	25	9	55	-18 ± 39	58	-53 ± 79	c	2	4	4
141	0917 + 624		1.45	1.2		1.6	123	10	132	-34 ± 13	129	31 ± 11	d	1	2	2
142	0919 − 260		2.30	2.4		1.2	336	13	62	3 ± 22	137	21 ± 31	o	2	1	1
143	0920 + 390						44	7	95	-91 ± 16	63	-13 ± 21	c		4	4
144	0920 − 397		.59	1.5		2.1	88	12	62	-17 ± 15	140	-227 ± 59	c		4	4
145	0923 + 392	4C39.25	.70	7.6		4.2	2756	13	296	52 ± 3	153	-11 ± 2	o	1	4	4
146	0925 − 203		.35	.7	.8		17	6	47	20 ± 31	44	29 ± 40	c		1	
147	0945 + 408		1.25	1.8		1.7	14	9	64	-17 ± 16	66	-14 ± 11	d	2	2	1
148	0951 + 693	M81		.1		.5	65	9	127	3 ± 25	164	-10 ± 25	o		2	2
149	0952 + 179		1.48	.7		1.0	33	10	64	-38 ± 12	74	39 ± 23	d	3	2	2
150	0953 + 254	OK290	.71	1.8		1.3	530	13	284	38 ± 18	219	49 ± 15	o	1	3	3

(continued on next page)

(Table 4. continued)

No	Source	Alter.	Redsh.	Flux (Jy) 6 cm	11 cm	15 cm	Number sess	pts	R.A. cos(δ) AlSd μas	Drift μas/year	Declination AlSd μas	Drift μas/year	Stability criteria 1	2	3	4
151	0954+658		.37	1.5		.9	247	12	90	1 ± 8	113	-31 ± 17	d	1	2	2
152	0955+326		.53	.7		.7	13	8	70	0 ± 4	126	9 ± 6	d	2	1	1
153	0955+476		1.87	1.0		1.1	1049	11	329	-33 ± 4	119	2 ± 2	d	1	4	4
154	1004+141		2.71	.7		.8	262	13	145	16 ± 23	98	18 ± 13	o	2	2	2
155	1012+232		.56	1.1	.7		13	7	27	27 ± 19	53	13 ± 30	d	1	1	1
156	1014+615		2.80				19	7	225	-128 ± 47	50	-43 ± 8	c		4	4
157	1020+400		1.25	.9		1.2	15	10	219	-10 ± 2	35	-27 ± 6	d	1	3	2
158	1022+194		.83	.6		1.0	22	6	43	-12 ± 13	172	94 ± 61	c	2	4	
159	1030+415		1.12	1.1		.8	15	6	58	-122 ± 28	29	-53 ± 20	d	2	4	
160	1032–199		2.20	1.0	1.1		11	8	146	305 ± 42	196	-222 ± 76	d		4	
161	1034–293		.31	1.5		1.3	1081	13	113	-9 ± 7	138	8 ± 11	o	1	2	2
162	1038+064		1.26	1.3		1.6	48	11	74	-58 ± 17	119	125 ± 51	d	1	4	4
163	1038+528	1038+52*A*	.68	.7	.4		162	10	59	-13 ± 10	168	39 ± 24	d		2	2
164	1039+811		1.26	1.1	.9		37	11	41	4 ± 10	53	-3 ± 14	d	1	1	1
165	1044+719		1.15	.7		1.0	508	12	240	-19 ± 12	204	5 ± 12	c	1	2	2
166	1045–188		.60	1.1	.9		12	7	5	-13 ± 2	18	-34 ± 4	o	1	2	
167	1053+704		2.49	.7		.6	27	9	111	-1 ± 21	34	-20 ± 3	c	1	2	2
168	1053+815		.71	.8		.6	179	12	75	-6 ± 5	114	8 ± 6	d	1	1	1
169	1055+018		.89	3.4		2.9	258	12	125	-3 ± 11	95	13 ± 13	o	2	2	2
170	1057–797						249	13	120	-11 ± 11	162	-24 ± 12	d		2	2
171	1101+384		.03	.7		1.0	209	9	138	-36 ± 11	78	5 ± 11	c	1	2	2
172	1101–536						33	8	63	77 ± 8	136	139 ± 47	c		4	4
173	1104–445		1.60	2.0	1.8		203	12	122	-119 ± 19	87	70 ± 27	o		4	
174	1111+149		.87	.5	.6		20	9	35	-20 ± 21	50	46 ± 30	d	1	1	1
175	1123+264		2.34	.8		.7	129	9	71	-9 ± 24	52	6 ± 13	o	1	1	1
176	1124–186		1.05	1.6		.6	405	12	64	5 ± 7	52	-8 ± 7	c	1	1	1
177	1127–145		1.19	7.3	6.4		28	9	200	-84 ± 85	43	45 ± 27	c	2	4	4
178	1128+385		1.73	.8		.9	707	12	85	-13 ± 3	138	6 ± 6	d	1	2	2
179	1130+009					.3	28	12	120	43 ± 67	88	-11 ± 73	d	1	1	
180	1144+402		1.09	1.0		.9	120	12	88	5 ± 7	129	-40 ± 13	o	1	2	2
181	1144–379		1.05	2.2	1.1		393	13	65	1 ± 8	85	50 ± 12	c		4	2
182	1145–071		1.34	1.2		1.0	114	10	64	-27 ± 11	121	-2 ± 19	c	1	2	2
183	1148–001		1.98	1.9		2.5	21	9	86	-103 ± 50	74	-119 ± 52	c	3	4	
184	1150+812		1.25	1.2		1.2	60	10	75	13 ± 8	110	20 ± 9	d	2	2	
185	1156+295		.73	1.5		1.3	589	13	125	-16 ± 4	205	-2 ± 7	c	2	2	2
186	1213+350		.86	1.0		1.2	16	8	44	-58 ± 22	21	6 ± 13	d	1	4	4
187	1213–172					1.2	18	8	160	36 ± 10	347	-93 ± 44	c	1	4	
188	1216+487		1.08	1.1		.7	15	9	28	-1 ± 21	42	-2 ± 23	d	1	1	1
189	1219+044		.96	1.4		.6	836	11	32	2 ± 2	157	-10 ± 9	d	1	1	1
190	1219+285		.10	.7		1.5	18	9	84	15 ± 37	54	-24 ± 24	c	2	1	
191	1221+809			.5	.4		19	10	62	-36 ± 9	35	-18 ± 4	d	1	2	2
192	1222+037		.96	1.2		1.0	53	10	71	56 ± 21	56	-82 ± 27	c	2	4	4
193	1226+023	3C273B	.16	43.4	41.4		1012	9	101	-227 ± 58	48	-137 ± 21	o		4	
194	1226+373		1.51	.9	.2		13	7	162	17 ± 46	180	-69 ± 62	d	1	4	
195	1228+126	3C274	.00	71.9			407	12	90	-10 ± 7	118	2 ± 9	c	3	1	1
196	1236+077		.40	.7		.6	16	8	58	-1 ± 40	108	157 ± 56	d	1	4	4
197	1237–101		.75	1.5		1.6	21	6	31	6 ± 22	104	129 ± 21	c		4	
198	1243–072		1.29	.9		.7	31	7	77	-83 ± 12	90	-39 ± 71	c	1	4	
199	1244–255		.64	2.3		1.4	76	10	125	2 ± 30	48	-44 ± 14	c		2	4
200	1251–713						18	7	53	-51 ± 43	73	-123 ± 51	d		4	

(continued on next page)

(Table 4. continued)

No	Source	Alter.	Redsh.	Flux (Jy) 6 cm	11 cm	15 cm	Number sess	pts	R.A. cos(δ) AlSd μas	Drift μas/year	Declination AlSd μas	Drift μas/year	Stability criteria 1	2	3	4
201	1252 + 119		.87	.7		1.8	35	7	37	70 ± 25	32	-5 ± 29	d	1	4	4
202	1253 − 055	3C279	.54	15.3		11.8	223	11	202	195 ± 32	152	-72 ± 33	o	2	4	4
203	1255 − 316		1.92	1.4		1.6	144	11	77	65 ± 24	69	122 ± 23	c		4	4
204	1257 + 145					2.9	14	8	123	-181 ± 80	100	148 ± 74	d	1	4	
205	1300 + 580						197	9	89	-12 ± 6	45	-1 ± 5	o	1	1	1
206	1302 − 102		.29	.8		1.0	48	11	95	83 ± 16	109	120 ± 44	c	1	4	4
207	1308 + 326		1.00	1.5	1.6		1314	13	233	-3 ± 10	232	17 ± 10	d	1	2	2
208	1308 + 328		1.65	1.1			34	7	66	22 ± 17	127	72 ± 25	n		4	4
209	1313 − 333		1.21	1.1		1.2	177	11	35	-4 ± 10	132	-19 ± 50	c	1	1	1
210	1315 + 346	OP326	1.05	.3	.5		21	10	75	7 ± 10	53	-39 ± 17	c	1	1	
211	1334 − 127		.54	2.8		1.9	1670	13	183	-18 ± 6	108	-10 ± 6	o	1	2	2
212	1342 + 663		1.35	.8	.6		39	10	60	5 ± 13	84	-19 ± 17	d	1	1	1
213	1347 + 539		.98	1.0		.9	14	9	117	-117 ± 35	118	-32 ± 19	d	2	4	
214	1349 − 439		.05	.8	.5		21	9	27	-17 ± 42	30	33 ± 42	c		1	
215	1351 − 018		3.71	.8		.8	434	11	121	6 ± 8	111	34 ± 10	c	1	2	2
216	1354 + 195		.72	2.6		1.8	124	12	104	12 ± 12	107	16 ± 18	o	2	2	2
217	1354 − 152		1.89	.8		1.2	91	10	378	-8 ± 68	430	82 ±116	c	1	4	4
218	1357 + 769						861	11	98	-1 ± 3	116	5 ± 2	c	1	1	1
219	1402 + 044		3.21	.7		.6	41	8	253	17 ± 46	201	-34 ± 71	c	1	2	2
220	1404 + 286	OQ208	.08	2.9		1.7	1156	12	39	2 ± 2	139	47 ± 5	o	1	2	2
221	1406 − 076		1.49	.8		1.3	31	10	32	-9 ± 12	33	31 ± 17	c	1	1	
222	1413 + 135		.25	1.2		.9	36	12	81	19 ± 12	59	36 ± 16	o	3	2	2
223	1418 + 546		.15	1.1		1.0	356	12	129	-7 ± 5	109	9 ± 4	d	2	2	2
224	1424 − 418		1.52	2.2		2.2	296	13	82	-23 ± 12	125	-8 ± 23	o		2	2
225	1435 + 638		2.07	.8		1.6	15	8	51	54 ± 23	40	-4 ± 34	d	3	4	4
226	1442 + 101	OQ172	3.54	1.1		2.0	30	9	156	31 ±103	103	9 ± 62	d	3	2	2
227	1448 + 762		.90	.7		1.0	21	8	45	-72 ± 31	89	-41 ± 28	d	1	4	4
228	1451 − 375		.31	1.8		1.4	114	11	103	-34 ± 17	107	-22 ± 49	c		2	2
229	1451 − 400		1.81	.6	.7		27	7	133	-3 ± 57	78	24 ± 49	c		1	1
230	1458 + 718	3C309.1	.90	3.8		6.9	18	9	69	36 ± 18	132	-188 ± 33	o	3	4	4
231	1459 + 480					.5	12	7	20	25 ± 12	20	20 ± 17	d	1	2	2
232	1502 + 106		1.83	2.5		2.0	567	10	132	-25 ± 14	45	17 ± 3	o	1	2	2
233	1504 − 166		.88	2.8		2.2	29	6	90	16 ± 76	80	11 ± 55	c	1	1	1
234	1508 + 572		4.30	.3			51	7	80	-52 ± 15	109	-37 ± 22	c		4	4
235	1510 − 089		.36	4.4		3.1	315	11	166	-4 ± 13	127	-17 ± 12	o	1	2	2
236	1511 − 100		1.51	1.2		.9	19	8	210	-97 ± 31	90	-4 ± 57	c	1	4	
237	1514 + 197		1.07	.5		.5	12	8	37	-8 ± 5	62	28 ± 10	d	1	1	
238	1514 − 241		.05	1.9		1.9	215	10	96	-31 ± 14	69	6 ± 22	c		1	2
239	1519 − 273			1.8		1.0	183	11	112	-11 ± 10	110	-8 ± 11	c		2	2
240	1538 + 149		.61	2.0		1.5	35	8	133	-24 ± 38	165	23 ± 49	d	1	2	2
241	1546 + 027		.41	1.1		.8	41	11	96	22 ± 16	154	12 ± 57	c	1	2	2
242	1547 + 507		2.17	.7	.7		14	6	28	45 ± 18	28	31 ± 20	d	3	2	1
243	1548 + 056		1.42	2.2		2.3	216	11	83	-33 ± 12	104	125 ± 21	o	2	4	4
244	1557 + 032		3.89	.5	.5		27	6	174	-12 ± 43	355	35 ±152	c		4	4
245	1600 + 335					2.7	16	6	213	21 ± 12	61	38 ± 12	d	1	2	2
246	1604 − 333					.6	20	8	48	56 ± 50	110	22 ± 71	d		4	
247	1606 + 106		1.23	1.4		1.0	1211	13	190	21 ± 4	195	1 ± 5	d	1	2	2
248	1610 − 771		1.71	5.6	3.8		260	13	155	36 ± 29	229	10 ± 28	o		2	2
249	1611 + 343		1.40	2.3	2.4		1055	13	119	-11 ± 2	182	14 ± 5	c	1	2	2
250	1614 + 051		3.22	.9		.6	117	10	72	15 ± 13	104	-25 ± 28	c	1	2	2

(continued on next page)

(Table 4. continued)

No	Source	Alter.	Redsh.	Flux (Jy) 6 cm	11 cm	15 cm	Number sess	pts	R.A. cos(δ) AlSd μas	Drift μas/year	Declination AlSd μas	Drift μas/year	Stability criteria 1	2	3	4
251	1622 − 253		.79	2.2	2.3		1246	13	89	-3 ± 5	82	-18 ± 7	o	1	1	1
252	1622 − 297		.81	1.9		2.2	41	9	72	18 ± 43	58	-22 ± 44	c		1	1
253	1624 + 416		2.55	1.6		1.5	31	10	78	7 ± 19	118	-7 ± 30	d	2	1	1
254	1633 + 382	1633+38	1.81	4.1		2.1	433	11	146	15 ± 12	128	5 ± 12	o	1	2	2
255	1637 + 574		.75	1.8		1.4	258	12	102	6 ± 10	123	17 ± 19	d	1	2	2
256	1638 + 398	NRAO512	1.67	1.2		1.1	814	12	169	-11 ± 8	115	23 ± 4	o	1	2	2
257	1641 + 399	3C345	.59	5.7		7.6	1087	10	335	85 ± 44	210	75 ± 9	o	1	4	4
258	1642 + 690		.75	1.4		1.7	146	11	86	4 ± 5	64	23 ± 5	d	2	2	2
259	1652 + 398	DA426	.03	1.3	1.5		207	11	57	-2 ± 6	89	34 ± 10	c	2	2	2
260	1655 + 077		.62	1.6		1.6	18	9	62	-23 ± 18	63	28 ± 38	c	3	1	1
261	1656 + 053		.88	1.4		1.6	45	9	1304	205 ± 45	294	22 ± 6	c	2	4	4
262	1657 − 261					1.1	30	10	39	43 ± 16	97	45 ±106	c		1	
263	1705 + 018		2.58	.5	.5		42	9	48	15 ± 10	48	85 ± 16	d	1	4	4
264	1706 − 174						37	11	66	-49 ± 36	73	-52 ± 53	d	1	4	
265	1717 + 178			.9		1.0	15	8	83	25 ± 21	31	-6 ± 16	o	1	1	1
266	1725 + 044		.29	.9		.8	15	11	81	43 ± 23	147	-41 ± 75	d	1	2	4
267	1726 + 455		.71	.6	.7		755	11	176	-17 ± 7	89	14 ± 3	d	1	2	2
268	1730 − 130	NRAO530	.90	4.2	4.9		599	11	90	20 ± 12	144	71 ± 26	o	2	4	4
269	1732 + 389		.98	1.1	.7		41	7	95	9 ± 4	129	-1 ± 16	c	1	1	4
270	1738 + 476		.32	.9		.9	18	9	46	-41 ± 8	28	5 ± 10	c	1	2	2
271	1739 + 522		1.38	2.0	1.9		1366	13	303	-3 ± 6	344	-1 ± 7	c	1	4	4
272	1741 − 038		1.06	2.3		5.6	2158	13	212	-18 ± 4	146	16 ± 4	o	1	3	3
273	1743 + 173		1.70	.9		.9	29	8	116	-36 ± 17	264	25 ± 12	d	1	2	4
274	1745 + 624		3.89	.6	.6		411	10	138	3 ± 9	103	-10 ± 7	d	2	2	2
275	1749 + 096		.32	2.5		1.1	1545	13	189	5 ± 4	203	-3 ± 6	c	1	2	2
276	1749 + 701		.77	1.1		1.1	20	6	36	63 ± 16	76	-42 ± 18	d	2	4	4
277	1751 + 288					1.1	16	6	17	25 ± 9	24	-45 ± 29	o	1	2	
278	1758 + 388		2.09	.9		.6	24	8	97	10 ± 17	124	-61 ± 15	c		4	4
279	1800 + 440		.66	1.0		.8	12	6	56	-79 ± 23	24	-60 ± 9	d	1	4	
280	1803 + 784		.68	2.6		2.6	1942	13	199	-3 ± 3	152	0 ± 3	c	1	2	2
281	1806 + 456		.83	.7		.5	12	7	92	-77 ± 52	32	-32 ± 15	c		4	
282	1807 + 698	3C371	.05	1.7		3.1	249	13	71	12 ± 3	84	7 ± 4	c	2	2	2
283	1815 − 553						145	13	103	33 ± 39	102	23 ± 24	o		2	2
284	1821 + 107		1.36	1.2	.9		19	8	39	47 ± 26	34	36 ± 29	c	1	2	
285	1823 + 568		.66	1.7		1.6	164	11	98	-1 ± 8	93	23 ± 8	d	1	1	1
286	1830 + 285		.59	1.0		1.3	11	7	62	5 ± 23	27	3 ± 20	d	2	1	1
287	1831 − 711		1.36	1.1	1.3		19	8	102	151 ± 39	9	3 ± 8	c		4	4
288	1842 + 681		.47	.9		1.2	12	8	58	37 ± 22	60	44 ± 17	d	1	2	2
289	1845 + 797	3C390.3	.06	4.5		7.3	29	11	170	65 ± 57	187	26 ± 55	d	2	4	4
290	1849 + 670		.66	.6	.9		121	7	31	-31 ± 8	74	63 ± 6	d	2	4	4
291	1856 + 737	1856+736	.46	.4	.4		13	7	36	37 ± 12	48	-69 ± 10	d	1	4	
292	1901 + 319	3C395	.63	1.8		3.1	28	10	184	-67 ± 28	119	68 ± 25	o	3	4	4
293	1908 − 201					2.3	387	12	60	0 ± 8	172	-25 ± 18	c		2	2
294	1920 − 211						63	10	124	10 ± 26	197	53 ± 49	c		4	2
295	1921 − 293		.35	14.3	4.6		1358	13	123	1 ± 7	185	-37 ± 16	o	1	2	2
296	1923 + 210						97	10	59	-42 ± 18	47	-30 ± 12	c	2	2	2
297	1928 + 738		.30	3.3		3.0	129	11	99	-20 ± 10	170	-11 ± 16	o	2	2	2
298	1933 − 400		.96	1.4	1.2		26	10	33	5 ± 11	34	-33 ± 26	c		1	
299	1936 − 155		1.66	.8		1.3	46	9	66	17 ± 18	109	36 ± 30	c	1	2	2
300	1937 − 101		3.79	.8		.9	16	9	170	-17 ± 20	43	-31 ± 20	c	1	2	2

(continued on next page)

(Table 4. continued)

No	Source	Alter.	Redsh.	Flux (Jy) 6 cm	11 cm	15 cm	Number sess	pts	R.A. cos(δ) AlSd μas	Drift μas/year	Declination AlSd μas	Drift μas/year	Stability criteria 1	2	3	4
301	1947+079		2.70	.7		.5	28	6	112	87 ±279	175	935 ±239	n		4	4
302	1954+513		1.22	1.6		1.4	43	10	40	3 ± 10	45	-18 ± 12	d	1	1	1
303	1954–388		.63	2.0		1.0	373	11	56	12 ± 10	88	-34 ± 20	d		2	2
304	1958–179		.65	2.7		1.1	839	13	98	4 ± 4	90	2 ± 6	o	1	1	1
305	2000–330		3.78	1.0		1.1	21	9	85	-125 ± 56	107	27 ±155	d		4	
306	2007+777		.34	1.3		1.2	241	11	303	45 ± 13	56	3 ± 3	o	1	4	4
307	2008–159		1.18	.9		.6	84	11	88	15 ± 15	139	-72 ± 33	o	1	4	
308	2021+317						13	8	35	-35 ± 24	42	16 ± 24	d	1	1	
309	2029+121		1.22	1.3		1.1	20	8	34	-10 ± 13	38	-54 ± 30	d	1	4	4
310	2037+511	3C418	1.69	3.8		5.0	353	12	54	0 ± 3	45	1 ± 3	d	3	1	1
311	2037–253		1.57	.7		.9	11	6	66	184 ± 19	63	-149 ± 29	c		4	
312	2052–474		1.49	2.5	3.0		70	12	106	-22 ± 31	111	-22 ± 49	d		2	4
313	2059+034		1.01	1.4		.6	12	10	48	-32 ± 8	63	-13 ± 20	d	1	2	4
314	2106–413		1.05	2.3	2.1		22	9	123	79 ± 28	59	-21 ± 25	d		4	
315	2109–811						14	5	18	-50 ± 30	78	152 ±148	d		4	
316	2113+293		1.51	1.5		1.1	139	11	61	-8 ± 5	371	15 ± 34	d	1	3	3
317	2121+053		1.94	3.2		2.5	851	13	397	78 ± 10	73	-1 ± 3	o	1	4	4
318	2126–158		3.28	1.2		.9	180	12	96	6 ± 13	70	-74 ± 15	c	1	4	4
319	2128–123		.50	2.0		1.7	700	12	249	37 ± 27	234	20 ± 47	o	2	2	2
320	2131–021		1.28	2.1		2.2	15	8	19	-63 ± 4	22	99 ± 16	c	1	4	
321	2134+004	2134+00	1.93	11.5		6.5	909	13	70	-38 ± 18	94	-40 ± 26	o	1	2	2
322	2136+141		2.43	1.1		1.2	278	12	122	24 ± 9	49	-19 ± 5	d	1	2	2
323	2143–156		.70	.5		1.0	18	9	84	17 ± 17	213	-55 ±109	d	2	4	
324	2144+092		1.11	1.0		.8	24	9	507	35 ± 9	142	-29 ± 15	c	1	4	
325	2145+067		1.00	4.4		3.1	1696	13	439	-5 ± 14	180	22 ± 7	d	1	4	4
326	2149+056		.74	1.0		1.1	40	12	419	-72 ± 52	222	-46 ± 70	c	1	4	4
327	2149–307	2149–306	2.35	1.3		1.4	16	6	112	-21 ± 50	90	-4 ± 53	o		1	
328	2150+173			1.0		1.1	21	6	131	-57 ± 50	82	-30 ± 34	d	2	4	4
329	2155–152		.67	1.7		1.8	61	10	231	76 ± 67	166	193 ± 67	o	1	4	4
330	2200+420	VR422201	.07	2.9		4.2	955	12	134	-10 ± 6	268	0 ± 10	o	1	2	2
331	2201+315		.30	2.8		2.0	305	13	167	11 ± 8	296	32 ± 12	o	1	2	2
332	2209+236					.7	18	11	69	42 ± 22	31	15 ± 12	d	1	2	2
333	2210–257		1.83	.8		.9	11	6	80	43 ± 11	71	-61 ± 15	c		4	
334	2216–038		.90	1.6		1.6	441	12	94	4 ± 8	211	24 ± 30	o	1	2	2
335	2223–052	3C446	1.40	4.1		5.2	248	9	165	36 ± 15	206	-73 ± 23	c	3	4	4
336	2227–088		1.56	1.4		1.3	61	11	153	52 ± 20	67	-63 ± 19	c	1	4	4
337	2229+695			.8	.6		18	9	82	-98 ± 36	59	-12 ± 25	d	1	4	4
338	2230+114	CTA102	1.04	4.0	4.9		158	12	185	21 ± 10	77	-18 ± 7	o	2	2	2
339	2232–488		.51	.9	.8		13	6	41	116 ± 46	44	-104 ±145	d		4	
340	2233–148		$\geq$ .61	.6	.5		18	9	72	77 ± 35	31	-97 ± 36	c	1	4	
341	2234+282		.80	1.1		.9	1689	13	384	-73 ± 9	264	-45 ± 6	c	1	4	4
342	2243–123		.63	2.7	2.7		369	12	113	26 ± 11	350	-88 ± 46	o	1	4	4
343	2245–328		2.27	.6	2.0		31	10	44	70 ± 20	58	-84 ± 45	c		4	
344	2251+158	3C454.3	.86	10.0		10.5	1067	10	296	-222 ± 58	73	5 ± 28	o		4	4
345	2253+417		1.48	1.0		1.5	40	9	48	-21 ± 11	78	42 ± 23	c	1	2	2
346	2254+024		2.09	.5	.5		23	9	116	71 ± 54	87	-118 ± 62	c	1	4	4
347	2254+074		.19	.5		.9	20	9	79	-69 ± 14	27	-16 ± 7	d	1	4	
348	2255–282		.93	2.1	1.4		886	13	124	-3 ± 9	100	-15 ± 11	o	2	2	2
349	2318+049		.62	1.0	1.2		125	11	103	12 ± 19	48	12 ± 28	c	1	1	1
350	2319+272		1.25	1.1		1.1	27	10	282	32 ± 42	176	88 ± 26	d	1	4	4

(continued on next page)

(Table 4. continued)

No	Source	Alter.	Redsh.	Flux (Jy) 6 cm	11 cm	15 cm	Number sess	pts	R.A. cos(δ) AlSd μas	Drift μas/year	Declination AlSd μas	Drift μas/year	Stability criteria 1	2	3	4
351	$2320-035$		1.41	.4		.8	66	11	79	40 ± 22	101	-92 ± 50	c	2	4	4
352	$2326-477$		1.31	2.1	2.4		28	7	141	-79 ±157	28	-69 ± 57	d		4	
353	$2328+107$		1.49	1.0		1.0	13	6	16	32 ± 20	53	115 ± 66	c	2	4	
354	$2329-162$		1.15	1.9		1.2	11	5	28	100 ± 27	37	-48 ± 40	d	2	4	
355	$2331-240$		.05	.9		.9	22	9	161	-102 ± 57	113	43 ± 54	c		4	
356	$2335-027$		1.07	.6		.6	28	10	74	14 ± 36	107	-14 ± 80	c	1	1	
357	$2337+264$					1.0	15	9	147	271 ± 44	197	308 ± 91	o	3	4	4
358	$2344+092$	2344+09A	.67	1.4		1.9	27	11	412	169 ± 94	507	203 ±162	c	2	4	4
359	$2345-167$		.58	3.5	4.1		130	10	147	16 ± 32	86	-94 ± 32	o	1	4	
360	$2351+456$		1.99	1.5	1.4		28	8	36	-15 ± 20	29	24 ± 20	o	2	1	2
361	$2355-106$		1.62	1.6	.5		139	11	161	6 ± 20	175	17 ± 40	c	1	2	2
362	$2356+385$		2.70	.7		.5	206	7	73	41 ± 4	141	-82 ± 11	c		4	4